

**KERNFORSCHUNGSZENTRUM**

**KARLSRUHE**

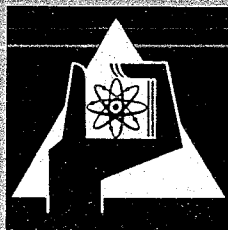
Oktober 1966

KFK 452  
CN-23/9

Institut für Angewandte Kernphysik

High-Resolution Cross-Section Measurements for Some Fast  
Reactor Structural Materials in the keV Energy Range

G. Rohr, E. Friedland, J. Nebe



GESELLSCHAFT FÜR KERNFORSCHUNG M. B. H.

KARLSRUHE



KERNFORSCHUNGSZENTRUM KARLSRUHE

October 1966

KFK 452

CN-23

Institut für Angewandte Kernphysik

High Resolution Cross-Section Measurement for  
Some Fast Reactor Structural Materials in the  
keV Energy Range

G. Rohr, E. Friedland, and J. Nebe

Gesellschaft für Kernforschung m.b.H. Karlsruhe



## 2. Experimental Method

Transmission measurements on  $^{51}\text{V}$ ,  $^{55}\text{Mn}$ ,  $^{57}\text{Fe}$  and natural iron were performed in the energy range of 20 to 220 keV by the time of flight method, using a pulsed 3 MeV van de Graaff accelerator having a pulse duration of 1 nsec. The neutrons were generated in a thick lithium target by means of the (p,n)-reaction. For energies up to about 50 keV a boron slab detector was used. In our detector the boron slab was surrounded by four heavily shielded NaI(Tl)-scintillation detectors connected in parallel, and mounted perpendicular to the neutron beam. This resulted in a background which was virtually time-uncorrelated and furthermore much lower than in the conventional setup, where the scintillator is placed directly behind the boron slab [1].

At higher energies it was advantageous to use a proton recoil detector. In this detector two multipliers in coincidence were coupled to the plastic scintillators in order to discriminate against multiplier noise.

The resolution of both spectrometers was determined from the measured time-width of the 478 keV  $\gamma$ -line originated in the target, and by furthermore taking into account the transit time spread of the neutrons through the detecting material and the channel width of the time analyser. The first mentioned time uncertainty was found as 2.8 nsec for the boron slab detector, which is about 30 % higher than for the detector with a single scintillator. In the case of the proton recoil detector this uncertainty was slightly energy dependent, changing from 3.9 to 3 nsec between 50 and 250 keV. The overall resolution was 0.39 nsec/m at 220 keV for a flight path of 10 meters.

## 3. Analysing technique

For analysis of the data the multilevel formula which results from the R-matrix formalism [2] was programmed for the IBM 7074 computer. An energy dependent correction term for the phase shift was assumed in order to approximate the influence of the unknown resonances outside the measured range [3]. This term

was found to change only slowly over the greatest part of the range, but was strongly energy dependent near the energy limits of the measured spectrum, showing the importance of outside resonances. The finite resolution of the spectrometer was accounted for by folding the multilevel formula with the experimental resolution function. This resolution function could be very well approximated by assuming a Gaussian form.

The programme is able to accommodate a maximum of 50 resonances for each spin system for a mixture of three different isotopes, considering s- and p-waves only. The computing time is about 10 min. for 100 points of the cross-section curve.

To extract the resonance parameters from the experimental cross-sections, tentative parameters were assigned to each peak for a first trial. The calculated cross-section curve was then compared with the experimental data and the parameters were adjusted till a satisfactory agreement was obtained.

#### 4. Results

For the interpretation of our data only s-waves were considered, as the p-wave strength function is a minimum in this mass region. Using the above mentioned method, it was thus possible to find parameters for all major resonances from 20 to 160 keV for  $^{51}\text{V}$  and from 50 to 210 keV for  $^{55}\text{Mn}$ . As the influence of neighbouring levels is strongly dependent on the spin state, it was in some cases even possible to assign unambiguous spin values to resonances who were far from resolved.

In table I all known parameters are given for  $^{51}\text{V}$ ; those determined before by Firk et al. [3] are marked by an asterisk.

For  $^{55}\text{Mn}$  the parameters of 42 resonances are tabulated in table II. The parameters for resonances up to 80 keV were determined before by Morgenstern et al. [4]; their results do not agree in all cases with ours.

The multilevel fit with our parameters is shown in fig. 1 and fig. 2. The solid line is the calculated cross section curve and the broken line represents the experimental values. The two curves show generally good agreement.

Fig. 3 shows the neutron cross-section for natural iron. No multilevel analysis has yet been made. The parameters in table III are found by area analysis.

As our spectrometer needs only small amounts of sample material, it is suited to investigate separated isotopes. Up to now only  $^{57}\text{Fe}$ , enriched to 90 %, has been measured. The cross-section is given in fig. 4. Analysis of these data is still in progress.

For  $^{55}\text{Mn}$  and  $^{51}\text{V}$  enough resonance widths have been measured to study the statistical behavior of them. One must keep in mind, however, that an appreciable number of small resonances are missed. In this sense a resonance is regarded as missed, if the width is too small for determining all the resonance parameters. If the resolution of the spectrometer is known, this number can be estimated under the assumption that their widths obey a Porter-Thomas distribution. Using the method of Fuketa and Harvey [5] we found for  $^{55}\text{Mn}$  that approximately 42 resonances with a reduced width smaller than  $1/5$  of the average value were missed. The resulting distribution function is shown in the lower diagram of fig. 5. Good agreement is found with the expected Porter-Thomas distribution.

In the case of  $^{51}\text{V}$  the same method yielded an unrealistic small number of about 5 missed resonances. Therefore the missed levels were estimated by counting every meaningful peak in the cross-section curve, giving a lower limit of 27 missed levels. The upper histogram in fig. 5 shows the result. It is obvious from this diagram that  $^{51}\text{V}$  does not obey a Porter-Thomas distribution. The reason for this might be the existence of broad doorway state resonances, which tend to shift the average width at too high values. This question, together with a discussion on the influence of ~~the~~ doorway-state resonances on other average nuclear properties, will be treated in more detail in a future publication.

References

- [1] GOOD, W.M., NEILER, J.H., and GIBBONS, J.H.,  
Phys. Rev. 109 (1958) 926
- [2] BOWMAN, C.D., BILPUCH, E.G., and NEWSON, H.W.,  
Ann. of Phys. 13 (1962) 319
- [3] FIRK, F.W.K., LYNN, J.E., and MOXON, M.C.,  
Proc. Phys. Soc. 82 (1963) 477
- [4] MORGENSTERN, J., DE BARROS, S., BIANCHI, G., CORGE, C.,  
HUYNH, V.D., JULIEN, J., LE POITTEVIN, G., NETTER, F.,  
et SAMCUR, C.,  
Int. Conf. on the Study of Nucl. Struct. with Neutrons,  
Antwerpen (1965) Paper 86.
- [5] FUKETA, T., and HARVEY, J.A., Nucl. Instr. and Meth. 33  
(1965) 107



TABLE I Resonance Parameters of  $^{51}\text{V}$

$E/\text{keV}$	$\Gamma_n/\text{keV}$	J	$E/\text{keV}$	$\Gamma_n/\text{keV}$	J
* 4.17	0.508 $\pm$ 0.006	4	68.1	4.70 $\pm$ 0.10	4
* 6.89	1.28 $\pm$ 0.014	3	83.0	1.20 $\pm$ 0.05	4
* 11.81	5.5 $\pm$ 0.05	3	87.6	3.20 $\pm$ 0.08	4
* 16.60	0.35 $\pm$ 0.04	4	110.8	0.25 $\pm$ 0.03	3
* 17.40	0.35 $\pm$ 0.04	4	113.5	0.11 $\pm$ 0.01	4
21.65	0.79 $\pm$ 0.05	3	114.8	0.08 $\pm$ 0.01	3
29.45	0.191 $\pm$ 0.02	4	116.6	2.40 $\pm$ 0.08	4
39.3	0.57 $\pm$ 0.04	3	118.7	20.5 $\pm$ 1.0	4
48.15	0.15 $\pm$ 0.02	4	118.7	0.13 $\pm$ 0.02	3
49.55	0.63 $\pm$ 0.04	3	134.7	3.20 $\pm$ 0.15	4
51.95	0.115 $\pm$ 0.02	4	141.3	3.60 $\pm$ 0.15	3
53.0	0.98 $\pm$ 0.04	3	145.7	1.50 $\pm$ 0.10	3
62.9	3.80 $\pm$ 0.10	3	152.9	3.50 $\pm$ 0.15	4

TABLE II Resonance Parameters of  $^{55}\text{Mn}$

$E/\text{keV}$	$\Gamma_n/\text{keV}$	J	$E/\text{keV}$	$\Gamma_n/\text{keV}$	J
53.4	0.09 $\pm$ 0.01	2	123.5	0.51 $\pm$ 0.05	2
57.45	0.81 $\pm$ 0.03	3	127.0	2.03 $\pm$ 0.20	3
58.0	0.06 $\pm$ 0.01	2	128.1	1.51 $\pm$ 0.15	2
59.5	0.27 $\pm$ 0.02	3	129.5	1.21 $\pm$ 0.15	2
59.95	0.10 $\pm$ 0.01	2	131.0	0.22 $\pm$ 0.03	3
64.1	1.01 $\pm$ 0.05	3	142.1	0.55 $\pm$ 0.06	3
66.6	0.16 $\pm$ 0.02	2	151.3	0.41 $\pm$ 0.08	2
69.55	0.14 $\pm$ 0.02	3	155.8	1.02 $\pm$ 0.10	2
70.07	0.32 $\pm$ 0.02	2	158.7	0.92 $\pm$ 0.05	3
73.9	0.71 $\pm$ 0.04	3	166.9	0.31 $\pm$ 0.05	2
81.3	0.44 $\pm$ 0.03	2	172.2	1.72 $\pm$ 0.15	3
84.35	1.31 $\pm$ 0.05	3	176.9	0.32 $\pm$ 0.03	3
96.05	0.21 $\pm$ 0.02	2	179.9	0.35 $\pm$ 0.05	2
98.2	0.45 $\pm$ 0.04	3	181.0	0.25 $\pm$ 0.05	3
103.7	0.27 $\pm$ 0.02	2	184.4	1.00 $\pm$ 0.15	2
104.9	1.51 $\pm$ 0.06	2	186.2	2.20 $\pm$ 0.20	3
107.0	0.41 $\pm$ 0.04	2	188.5	0.81 $\pm$ 0.10	3
109.4	1.32 $\pm$ 0.13	2	193.9	0.30 $\pm$ 0.03	3
110.9	1.83 $\pm$ 0.15	3	197.6	0.62 $\pm$ 0.05	2
116.1	0.47 $\pm$ 0.03	3	203.4	2.70 $\pm$ 0.30	3
118.4	0.71 $\pm$ 0.04	3	207.7	2.80 $\pm$ 0.30	2

TABLE III Resonance Parameter of  $^{56}\text{Fe}$

$E/\text{keV}$	$\Gamma_n/\text{keV}$	J	$E/\text{keV}$	$\Gamma_n/\text{keV}$	J
74.0	$0.539 \pm 0.042$	1/2	139.9	$2.460 \pm 0.110$	1/2
83.5	$0.912 \pm 0.085$	1/2	168.4	$0.874 \pm 0.074$	1/2
90.2	$< 0.050$	1/2	186.3	$3.425 \pm 0.267$	1/2
122.4	$0.125 \pm 0.023$	1/2	219.2	$1.470 \pm 0.085$	1/2
129.5	$0.479 \pm 0.038$	1/2	242.7	$0.630 \pm 0.042$	1/2



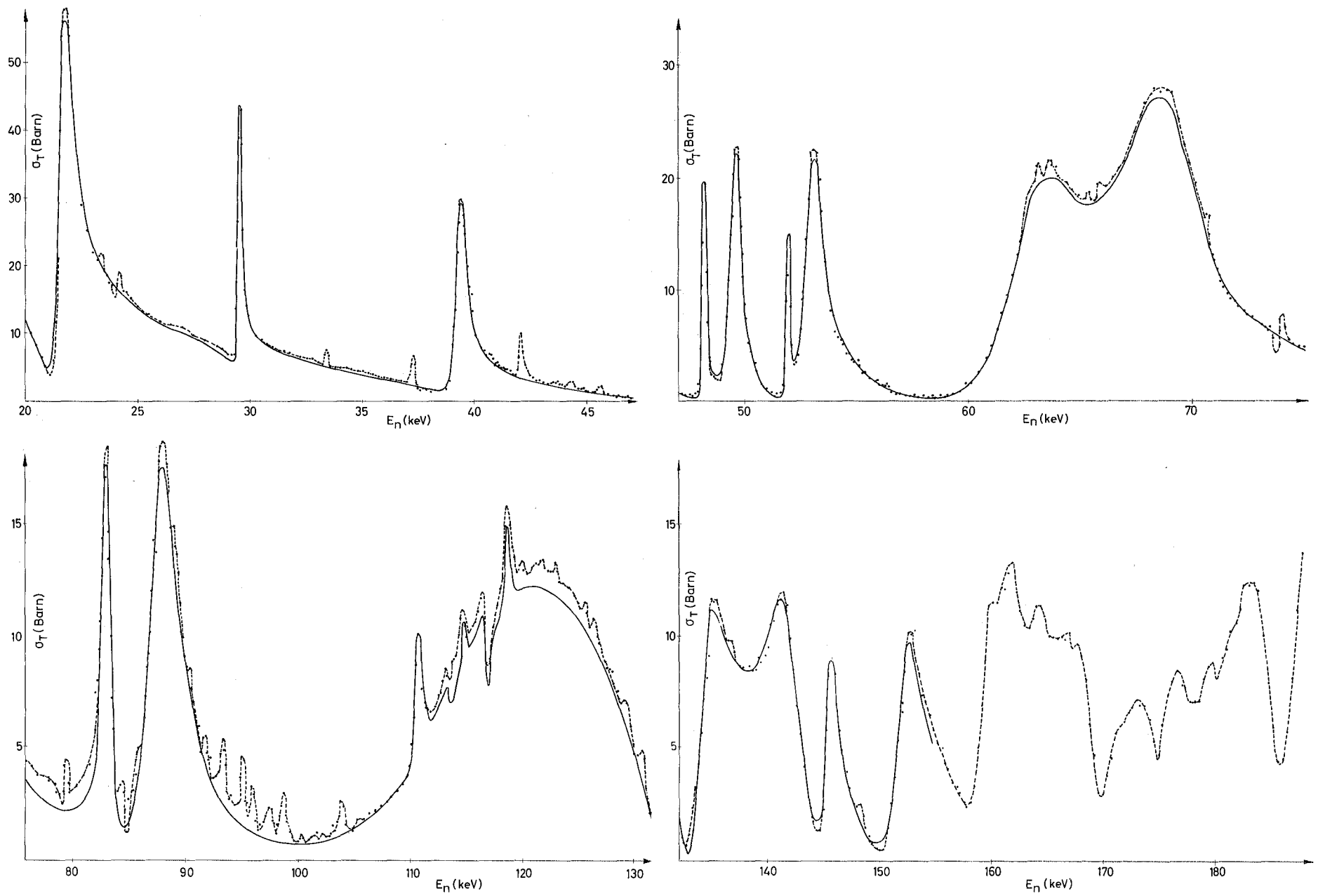


Fig.1 Total neutron cross section curve for  $^{51}\text{V}$ . The solid line represents the multilevel fit.

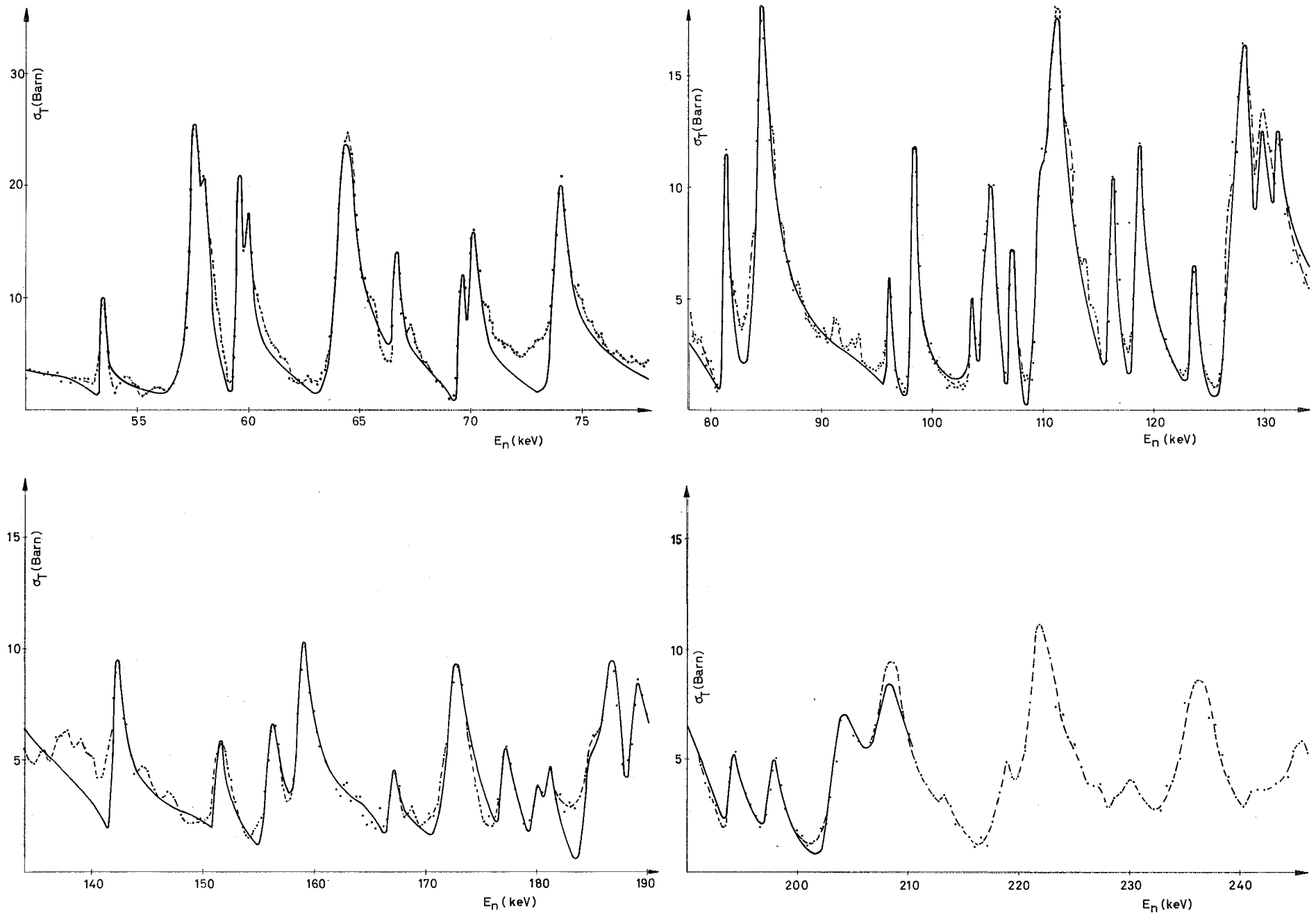


Fig. 2 Total neutron cross section curve for  $^{55}\text{Mn}$ . The solid line represents the multilevel fit.

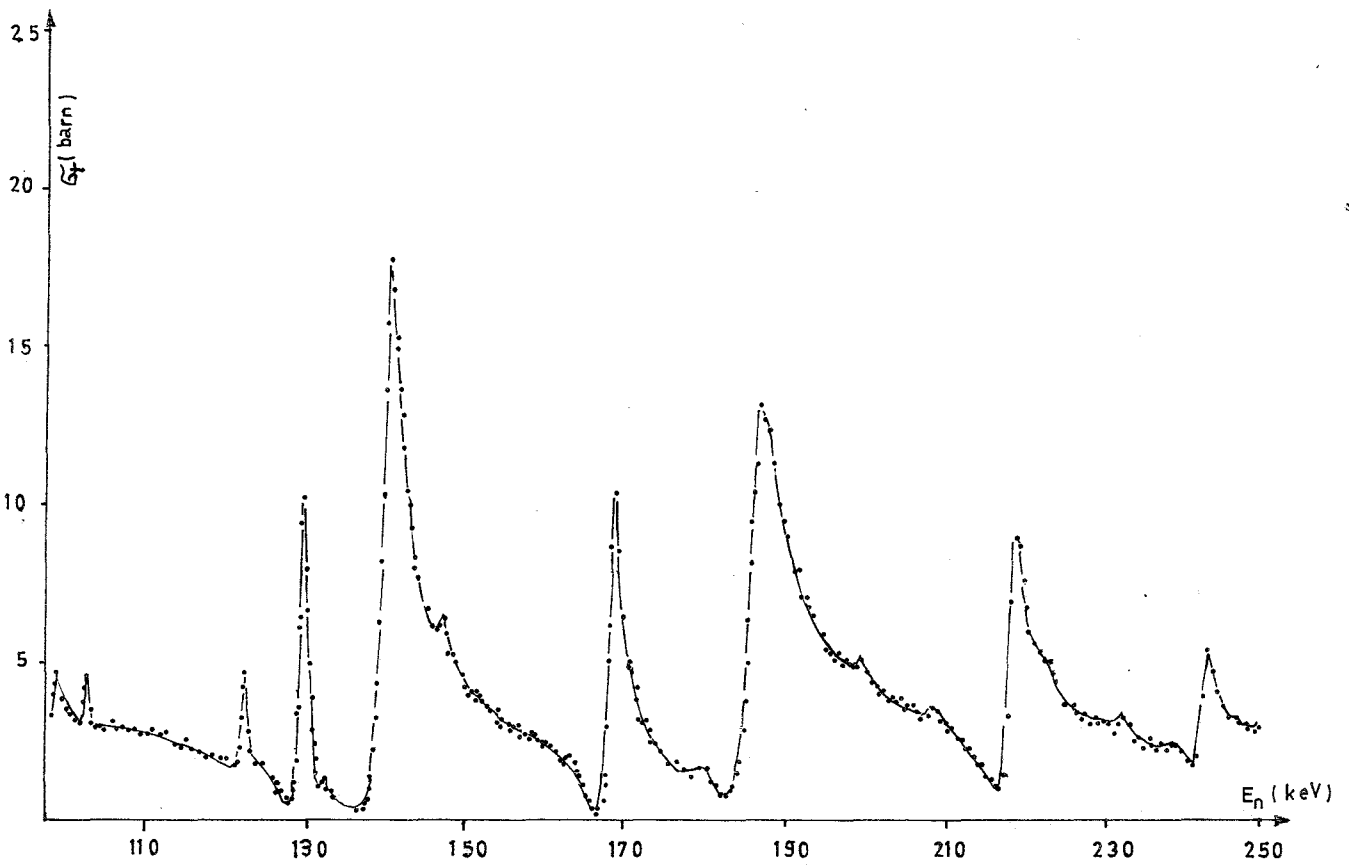
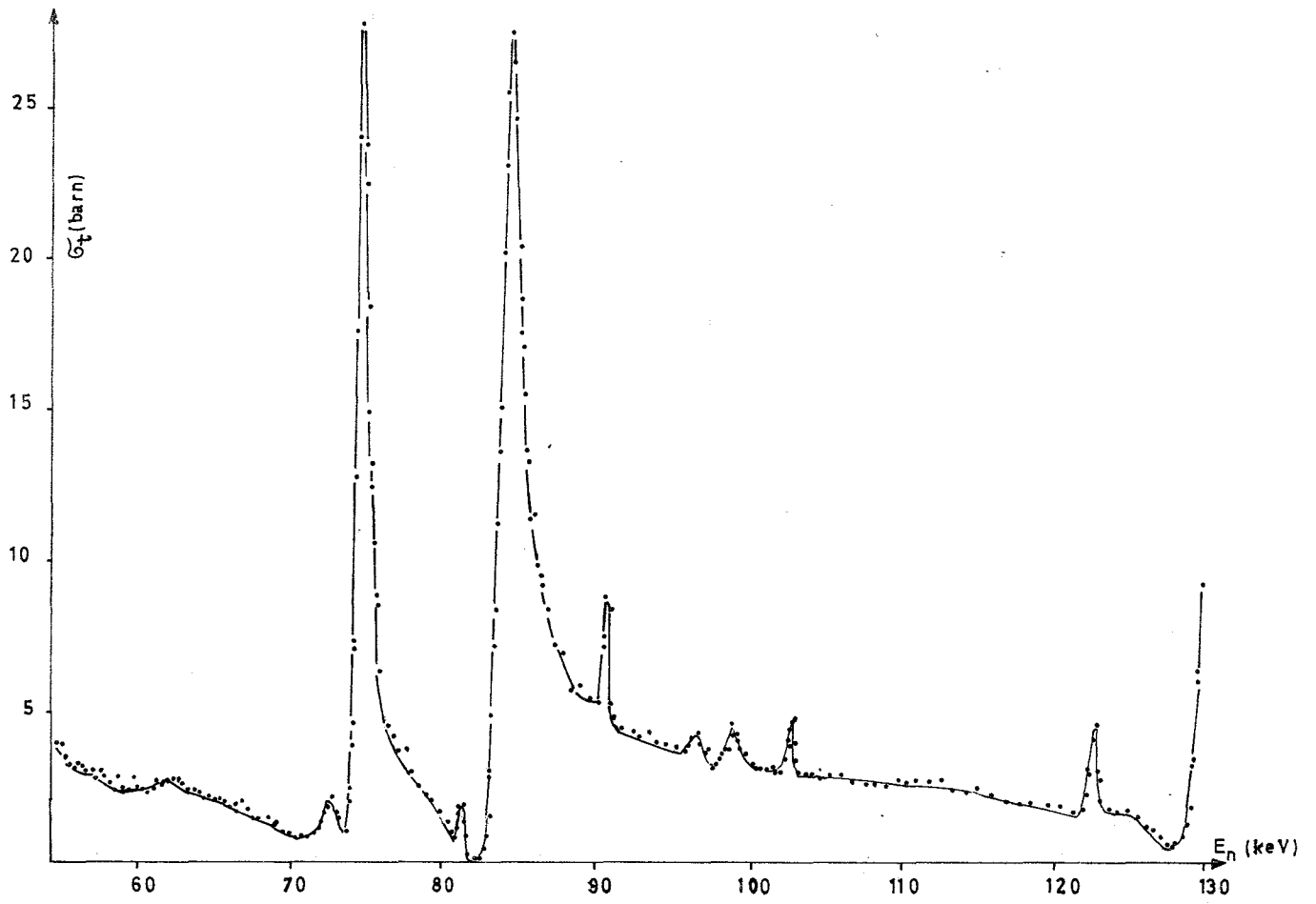


Fig.3 Total neutron cross section curve for natural iron.

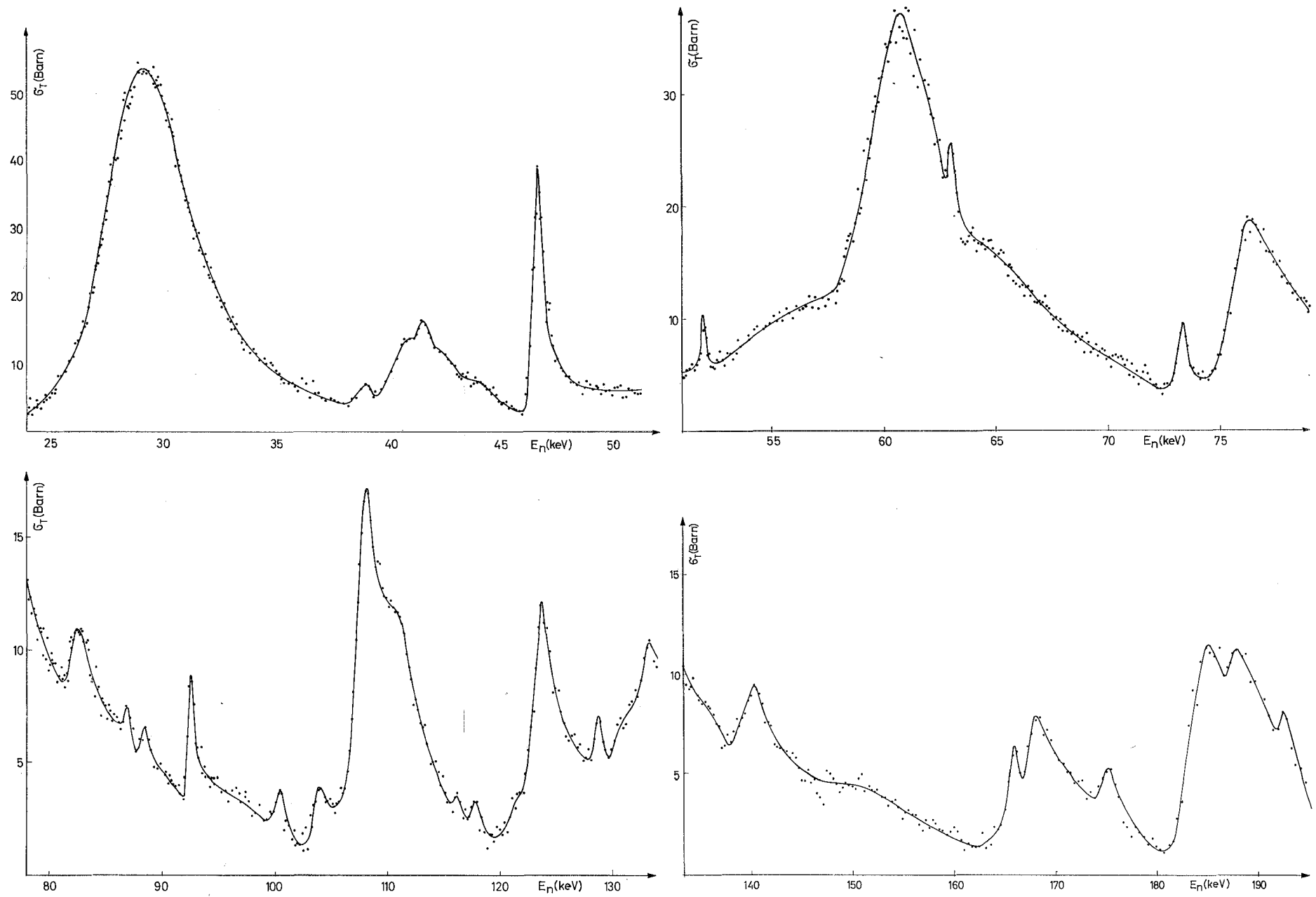


Fig.4 Total neutron cross section curve for  $^{56}\text{Fe}$ .

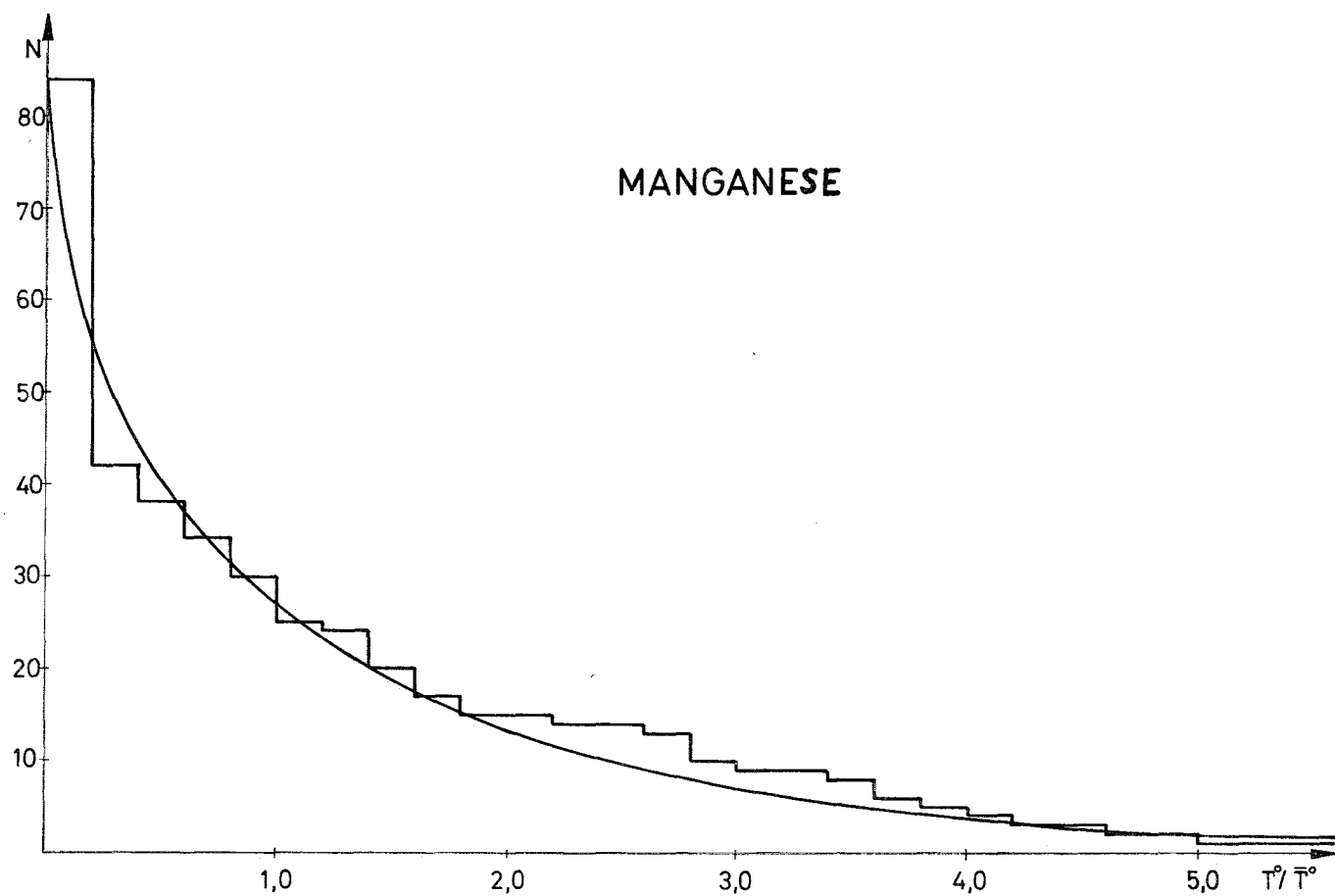
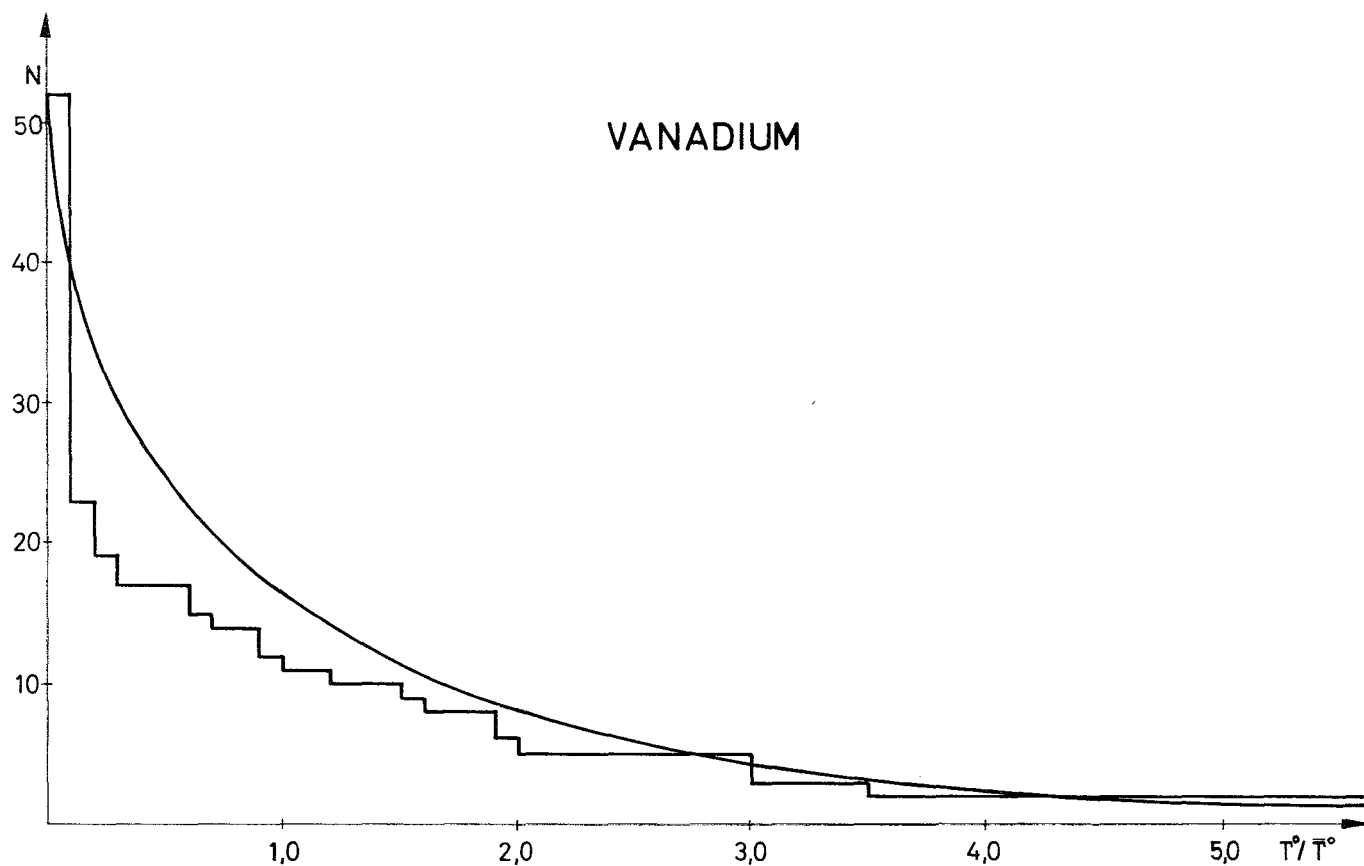


Fig. 5 Number of levels  $N$  with a normalized reduced width larger than  $\Gamma^\circ/\bar{\Gamma}^\circ$ .  
The smooth curve shows the Porter-Thomson distribution.